Response of microbial decomposition to spin-up explains CMIP5 soil carbon range until 2100

J.-F Exbrayat[1,2] A. J. Pitman[1] and G. Abramowitz[1]

[1]{ARC Centre of Excellence for Climate System Science and Climate Change Research Centre, University of New South Wales, Sydney, New South Wales, Australia}

[2]{School of GeoSciences and National Centre for Earth Observation, University of Edinburgh, Edinburgh, United Kingdom}

Correspondence to: J.-F. Exbrayat (j.exbrayat@ed.ac.uk)

Abstract

It has been reported that soil carbon storage simulated by the Coupled Model Intercomparison Project (CMIP5) models varies 6-fold for the present day. We show that this range already exists at the beginning of the historical simulations and demonstrate that it is mostly an artifact of the representation of microbial decomposition and its response during the spin-up procedure used by the models. The 6-fold range in soil carbon, once established, is maintained through the present and to 2100 almost unchanged even under a strong business-as-usual emissions scenario. By highlighting the role of the response of decomposition to spin-up in explaining why current CMIP5 soil carbon stores vary widely, we identify the need to better constrain the outcome of this procedure as a means to reduce uncertainty in transient simulations.

1 Introduction

The land surface currently absorbs about a third of anthropogenic emissions of CO_2 (Canadell et al., 2007; Le Quéré et al., 2009) and so helps to offset global warming. Future global warming may enhance microbial decomposition and emissions of CO_2 from respired soil organic carbon (*SOC*), the largest carbon pool in the terrestrial biosphere (Jobbágy and Jackson, 2000). Higher emissions from *SOC* could accelerate increases in atmospheric CO_2 concentrations even if plant carbon uptake

by photosynthesis increased under higher atmospheric CO_2 (Ahlström et al., 2013; Friedlingstein et al., 2014; Nishina et al., 2014). Conversely, if the soil remains a carbon sink (Le Quéré et al., 2009; Lund et al., 2010) the negative feedback on rising atmospheric CO_2 (Davidson and Janssens, 2006) would help limit rates of increase. How soil carbon is represented in models and how it responds to climate is critical to resolving whether the land will remain a sink or become a source of CO_2.

Recent model intercomparisons, such as the fifth phase the Coupled Model Intercomparison Project (CMIP5; Taylor et al., 2012), or the Inter-Sectoral Impact Model Intercomparison Project (ISI-MIP; Warszawski et al., 2013) have highlighted a lack of consensus among models on whether the soil carbon sink will be sustained during the 21st century (Friedlingstein et al., 2014; Nishina et al., 2014;). These models also exhibit large discrepancies in stores of *SOC* they simulate. For example, Todd-Brown et al. (2013) report that total *SOC* simulated by CMIP5 models for the present day represents a 6-fold variation ranging from ~510 to ~3040 Pg C. Another large range (~1090 to ~2645 Pg C) exists in the present day *SOC* simulated by ISI-MIP models despite being driven by a harmonized weather dataset (Nishina et al., 2014). These latter results indicate that a significant fraction of the uncertainty in estimates of total *SOC* arises from the representation of land processes rather than differences in climate drivers.

Soil carbon pools of widely different sizes have the potential to react differently to future climate change. We therefore examine the likely reasons for the large differences between CMIP5 models in their simulation of *SOC*. As noted by Knutti and Sedláček (2013) in the context of climate models, multiple sources of disagreement between models may exist such as a lack of process understanding, or the reduced availability of relevant observational datasets to constrain models. Discriminating between these sources of uncertainty to understand why CMIP5 models differ so significantly in the amount of *SOC*, and subsequently in the total amount of C mobilized in the global cycle, would enable an improvement in model projections of the resilience of *SOC* pools and improve our confidence in the sign of the soil carbon feedback in the future.

2 Material and methods

2.1 SOC in Earth System Models

In all global terrestrial models participating in recent intercomparison projects such as CMIP5 and ISI-MIP, the *SOC* balance and its change (ΔSOC) are derived in a similar way. First, inputs of carbon into the soil are derived from plant pools. Plant carbon uptake and turnover times respond to climate change, climate variability and atmospheric CO_2 independent of the size of the *SOC* pools. Meanwhile, modeled microbial decomposition releases carbon by heterotrophic respiration (R_h). The balance can be summarized by

$$\Delta SOC = SOC_{in} - R_h \quad (1)$$

where SOC_{in} is the input to the SOC pools from plant and litter pools.

Microbial decomposition is commonly represented as a first-order process and applied to a succession of pools. In each pool, a parameter k reflects the specific baseline residence time (Xia et al., 2013; Exbrayat et al., 2013a,b) at a reference soil temperature and non-limiting moisture conditions. Then, the decay rate is adjusted at each time step by an environmental scalar (Todd-Brown et al., 2013; Xia et al., 2013; Exbrayat et al., 2013a,b; Nishina et al., 2014) that describes the instantaneous response of microbial activity to the soil physical state as the product of a soil temperature (f_T) and a soil moisture respiration function (f_W). Various formulations of f_T and f_W have been implemented in model codes (Lloyd and Taylor, 1994; Falloon et al., 2011; Todd-Brown et al., 2013; Exbrayat et al., 2013a,b; Nishina et al., 2014) usually assuming a space and time-invariant response to the same conditions. Their effect on decay rate varies according to local soil conditions and therefore climate.

The actual decay rate ($k \times f_T \times f_W$) is applied to the amount of substrate available, SOC, to determine the amount of microbial decomposition D_m at each model time step:

$$D_m = k \times f_T \times f_W \times SOC \quad (2)$$

where $k \times f_T \times f_W$ is equivalent to the fraction of respired substrate, the inverse of the residence time SOC/R_h. A part of the decomposed organic matter is routed to pools with longer residence time and the rest is emitted as CO_2. There may be variations between models in the number of pools they represent (Todd-Brown et al., 2013; Nishina et al., 2014) and the formulations of the environmental

response functions (Falloon et al., 2011; Exbrayat et al., 2013a) but at the ecosystem scale, R_h is proportional to the amount of substrate, i.e. *SOC*, available in the soil. This parameterization may be inconsistent with our current understanding of microbial decomposition (Allison et al., 2010; Schmidt et al., 2011; Wieder et al., 2013) because it lacks the representation of processes like microbial activity and priming effect (e.g. Xenakis and Williams, 2014). However, the first-order dependency of R_h on *SOC*, soil temperature and moisture is able to explain complex phenomenon like the apparent acclimation of decomposers to warming by quick depletion of the most labile substrate pools (Luo et al., 2001; Kirschbaum, 2004; Knorr et al., 2005).

2.2 CMIP5 data

From the CMIP5 archive we downloaded monthly soil carbon density (*cSoil* in metadata), litter carbon density (*cLitter*) and heterotrophic respiration (*rh*) for 15 CMIP5 models from 10 international institutions. A list of models can be found in Table 1 while further details about models and land components have been summarized in Table 2. We note that four of these models, namely BCC-CSM1.1 (model A), CCSM4 (model C), NorESM1-M and NorESM1-ME (grouped as model J), represent nitrogen limitation on plant productivity while the others do not. We selected data for the historical (1850-2005) and the most intensive Representative Concentration Pathway 8.5 (RCP 8.5, 2006-2100) experiments. A total of 79 simulations for the historical experiment, including 34 simulations continuing for RCP 8.5 (Table 1) were available. When *cLitter* was reported, we added it to *cSoil* as both pools are parameterized to generate R_h following first-order kinetics.

To calculate stock sizes we first multiplied spatially explicit data of *cSoil* and *cLitter* in kg C m^{-2} by corresponding grid-cell areas (*areacella* in metadata) and integrated their values globally. Similarly, we calculated global fluxes of R_h by multiplying monthly fluxes in kg C m^{-2} by grid-cell areas and integrating them globally. Fluxes were summed to obtain annual averages. Annual soil carbon input (SOC_{in}) from above ground biomass was not available from the database. Therefore, we calculated it by inverting the *SOC* balance:

$$SOC_{in} = \Delta SOC + R_h \quad (3)$$

As models did not start their historical simulations at the same time, we focus our analyses on the overlapping period of 1861-2100. We also averaged all simulations from the same model or institution in an attempt to account for model dependence (see Bishop and Abramowitz, 2013, for a discussion on the topic).

In the following, we report values of stocks and fluxes averaged for three periods of time, the pre-industrial (1861-1870), modern (1996-2005) and future (2091-2100) periods. While the period 1861-1870 is not part of the pre-industrial control runs *sensu stricto*, the minor increase in atmospheric CO_2 between pre-industrial times (i.e. before 1850) and 1870 is unlikely to have led models to simulate a strong change in the greenhouse effect and terrestrial C fluxes. Values are shown in Table 3.

2.3 Harmonized World Soil Database

HWSD (FAO, 2012) is a global dataset of dominant soil units at a 30 second arc resolution, providing soil properties for the top (0-30 cm) and sub-soil (30-100 cm). We use version 1.21 and follow the approach by Todd-Brown et al. (2013) to obtain global values. First, we regridded the HWSD by selecting dominant soil units in a 0.5° latitude × 0.5° longitude grid. Then, we multiply the organic carbon content of the dominant soil units (in % weight) by the bulk density (provided in kg dm^{-3}) to obtain the carbon density (in kg C m^{-2}) in each 0.5° × 0.5° grid cell. We multiply the density by the surface area of each grid cell and sum results to obtain a total soil carbon content of ~1170 Pg C. Following Todd-Brown et al. (2013), a confidence interval of 29% below the mean (i.e. ~830 Pg C) to 32% above the mean (i.e. ~1550 Pg C) was considered to take variations in soil carbon content and the mapping processes into account. The range we obtain is slightly smaller than reported by Todd-Brown et al. (2013) (890 – 1660 Pg C) because we use an updated version of the HWSD and did not replace bulk density values for Andisols and Histosols.

3 Results

We first compare total *SOC* for pre-industrial (1861-1870), modern (1996-2005) and future (2091-2100) periods. Figure 1 compares the total *SOC* range in CMIP5 models for 1861-1870 (563 – 2938 Pg C), 1996-2005 (576 – 3047 Pg C), and 2096-2100 (582 – 3266 Pg C, derived using the RCP 8.5 scenario). All three periods show very similar distributions of *SOC* among the models and the present day and future ranges already exist at the beginning of the historical simulations. Figure 1 highlights that the size of SOC pools of individual CMIP5 models remain largely consistent over the three time periods. Indeed, pre-industrial *SOC* predicts modern *SOC*, modern *SOC* predicts future *SOC* and pre-industrial *SOC* predicts future stocks with a high degree of precision (Figure 1). Also represented in Figure 1 is the 95% confidence interval of total SOC estimated from HWSD that we use as a reference for modern total SOC (i.e. in 1996-2005). We note that only three models fall within this range: BCC-CSM1.1 (model A), CanESM2 (model B) and HadGEM2 (model F). Models based on the CLM4 land surface model (i.e. models C and J) underestimate modern *SOC* while all remaining models overestimate it. Note that these models C and J include nitrogen limitation of the vegetation response to increasing CO_2.

We next investigate the likely reasons for the existence of this pre-industrial CMIP5 range in total SOC. The first obvious step is to check whether models are at equilibrium prior to and climate change experiments. Models may not agree on total SOC simply because some of them, and especially those at the extremes of the CMIP5 spectrum, are still drifting toward their own steady-state and therefore do not comply with our experiment protocol. In Figure 2 we show the relationship between pre-industrial SOC_{in} and R_h. This relationship is highly significant ($R^2 = 1$; $p < 0.001$) and strongly suggests that all models were equilibrated under pre-industrial boundary conditions. This removes the possibility that models were not in equlibrium and means that the 6-fold CMIP5 range is likely linked with the internal terrestrial processes represented in these models.

Two major internal terrestrial processes are involved: SOC_{in}, the amount of SOC that enters the soil pools, and the residence time of organic matter that corresponds to the amount of SOC that is released from soil pools. The relationship between SOC_{in} and total *SOC* during the pre-industrial period is shown in Figure 3. Overall, the relationship is not significant (R^2=0.04; p=0.604). Further, the models that equilibrate with the largest total *SOC* stock (models E, H, I) are not the models with the largest SOC input. Similarly, the small equilibrated *SOC* pool size of models C and J seems

unrelated to SOC_{in} despite these models including N limitations on plant productivity and SOC_{in}. In short, the amount of SOC_{in} cannot explain the size of the initial pools. In Figure 4, we therefore present the relationship between the pre-industrial *SOC* residence time (i.e. the inverse of the decay rate expressed as SOC/R_h) and total *SOC*. This relationship is highly significant ($p < 0.001$) and linear ($R^2=0.84$) and models with a longer residence time, i.e. a low decay rate, require larger pools to offset the same SOC input, and vice-versa. Further, residence times are not affected by the number of SOC pools represented. Models with the longest residence time have alternatively 9 (model E) or 2 pools (models H and I), while models with the shortest residence time have 8 (model A), 6 (models C and J) or 4 pools (model F).

4 Discussion

Despite the change imposed on boundary conditions during global warming experiments (Anav et al., 2013; Friedlingstein et al., 2014), CMIP5 present day and projected *SOC* stocks are largely determined by their initial conditions (Figure 1). This was not unexpected due to the slow response of SOC pools but it clearly shows that modern and future stocks are defined by initial states. Further, as *SOC* in 1860 is unknown, CMIP5 models use a spin-up procedure assuming steady pre-industrial boundary conditions (Xia et al., 2012) to obtain an equilibrated state for pre-industrial *SOC*. In order to reach equilibrium, iterative or semi-analytical methods (e.g. Xia et al., 2012) are employed to reach the pool sizes required to balance input (SOC_{in}) and output fluxes (R_h). Steady-state is assumed when the trend in ΔSOC becomes negligible. Hence, it is not the actual value of *SOC* that defines the equilibrium but its lack of variation in time (Xia et al., 2013; Exbrayat et al., 2013b).

We have verified that all CMIP5 models were close to equilibrium prior to the initiation of climate change experiments. Following Equations 1 and 2, the model-specific value of *SOC* obtained by a model via spin-up depends on two factors. First, if SOC_{in} is large, a larger *SOC* pool is required to offset it through microbial decomposition and R_h, for a given decay rate, $k \times f_T \times f_W$. Conversely, low values of SOC_{in} lead *SOC* pools to equilibrate to lower values for a particular decay rate. Second, if the decay rate is high (short residence time) during spin-up, *SOC* pools will remain small, for a given SOC_{in}. Conversely, low decay rates, or long residence time, will require large pools of substrate to offset the same input SOC_{in}. Both factors are model-specific: SOC_{in} is derived from

196 plant primary productivity fluxes (Davidson and Janssens, 2006) while the baseline decay rate k and
197 the shape of the response functions f_T and f_W are highly model-dependent (Falloon et al., 2011;
198 Exbrayat et al., 2013a,b; Todd-Brown et al., 2013).

199 Here we have shown that the large range exhibited by CMIP5 *SOC* is principally due to the
200 response of microbial decomposition during the spin-up process (a long process that corresponds to
201 multiple centuries of steady climate conditions). Model-specific parameter k and environmental
202 response functions f_T and f_W drive SOC pools to the size required by the residence time they
203 simulate to compensate for SOC_{in}. This observation corroborates the predominance of residence
204 time in the uncertainty of ecosystem response to climate change (Friend et al., 2014) and Figure 4
205 shows that it is independent from the number of pools considered in each model. The resulting
206 equilibrated state obtained *prior* to the initiation of CMIP5 transient simulations propagates through
207 the present and into the future even when using RCP 8.5.

208 Our results raise a critical problem linked to model initialization by spin-up. According to our
209 analysis of the CMIP5 models, a simple solution to reduce the uncertainty in simulated *SOC* stocks
210 would be to modify model parameters, especially those related to *SOC* turn-over, to obtain a steady-
211 state with SOC values representative of pre-industrial conditions. Alternatively, because of the
212 millennial time-scales of soil genesis, as well as land use changes, steady-state of global SOC stocks
213 is not guaranteed to have existed at the end of the pre-industrial era. Therefore, one could choose to
214 only consider model parameters that achieve modern stocks in accordance with observations in
215 response to past changes (e.g. Exbrayat et al., 2014). However, this would require multiple
216 realisations of computationally expensive models, or the use of emulators. Therefore, as simulated
217 SOC does not vary much during historical experiments, we suggest that one could use available
218 estimates and confidence interval of modern SOC stocks such as those provided globally by HWSD
219 and other (Shangguan et al., 2014), and possibly incorporating regional data that may better
220 represent high latitude stocks and initial conditions for permafrost (e.g. Northern Circumpolar Soil
221 Carbon Database; Hugelius et al., 2013). Of course, while changing parameter values corresponding
222 to SOC residence time is relatively straightforward, it would be important to ensure that these pools
223 are sustained by an input representative of carbon uptake. At equilibirum SOC_{in} equals net primary
224 productivity (NPP) because plant pools do not vary in size. Here all models predict SOC_{in} within
225 two standard deviations of the uncertainty range of modern, high confidence, NPP estimates (56.4 ±

8–9 Pg C yr^{-1}; Ito et al., 2011). Although not directly comparable with pre-industrial values, this global estimate indicates that models simulate acceptable values of global carbon uptake.

As decomposition processes are represented following first-order kinetics, simulating more realistic initial *SOC* stocks in response to adequate uptake fluxes would likely lead models to represent more correct modern stocks. Nevertheless, as each model relies on its own formulation of the response functions f_T and f_W, the ensemble would still exhibit different sensitivities of SOC stocks to climate change. However, by removing a degree of freedom associated with initial conditions, we believe that these observational datasets are a valuable tool for improving the confidence we can have in projections of SOC fluxes and feedbacks on future climate change.

5 Conclusions

We have demonstrated that the 6-fold range in SOC stocks simulated by CMIP5 models can be explained by the model-specific response of microbial decomposition to spin-up under pre-industrial conditions. Model dependent parameter and response functions drive the size of the pools to the amount required by decay rates to offset SOC_{in} under the steady-state assumption. Once established, the resulting pool sizes remain similar through to the present and into the future even under the high-emissions RCP8.5 scenario that generates future conditions the least similar to current ones. We therefore identify the spin-up procedure, and especially the response of microbial decomposition during this very long model integration, as a key source of uncertainty in the simulation of *SOC* in CMIP5 models.

A model that equilibrates to a soil carbon store well outside the observed range should be examined with care. A very large amount of stored carbon increases the potential for the land surface to become a source as even a tiny relative change in decay rate can strongly enhance R_h and possibly reach a tipping point where it offset increases in SOC_{in}. Conversely, a very small *SOC* store increases the likelihood that it will remain a sink. Such results are likely to be artefacts of model implementation when *SOC* values are largely inconsistent with observed ranges.

In conclusion, we recommend that future intercomparisons should constrain model parameters so that each model achieves an equilibrated state similar to observations as the outcome of the spin-up

procedure. This would remove a degree of freedom in initial conditions when comparing differences in projected changes.

Acknowledgements

This work was supported by the Australian Research Council through grants DP110102618 and CE110001028. We thank P. Petrelli for the availability of CMIP5 data and the National Computational Infrastructure for data hosting and computational resources to process these model data. We thank Dr K. Todd-Brown for guidance in processing the HWSD database and Dr Y. Zhang for information about the BCC-CSM1.1 model.

We acknowledge the World Climate Research Programme's Working Group on Coupled Modelling, which is responsible for CMIP, and we thank the climate modeling groups (listed in Table 1 of this paper) for producing and making available their model output. For CMIP the U.S. Department of Energy's Program for Climate Model Diagnosis and Intercomparison provides coordinating support and led development of software infrastructure in partnership with the Global Organization for Earth System Science Portals.

References

Ahlström, A., Smith, B., Lindström, J., Rummukainen, M. and Uvo, C. B.: GCM characteristics explain the majority of uncertainty in projected 21st century terrestrial ecosystem carbon balance, Biogeosciences, 10(3), 1517–1528, doi:10.5194/bg-10-1517-2013, 2013.

Allison, S. D., Wallenstein, M. D. and Bradford, M. A.: Soil-carbon response to warming dependent on microbial physiology, Nat. Geosci., 3(5), 336–340, doi:10.1038/ngeo846, 2010.

Anav, A., Friedlingstein, P., Kidston, M., Bopp, L., Ciais, P., Cox, P., Jones, C., Jung, M., Myneni, R. and Zhu, Z.: Evaluating the Land and Ocean Components of the Global Carbon Cycle in the CMIP5 Earth System Models, J. Clim., 26(18), 6801–6843, doi:10.1175/JCLI-D-12-00417.1, 2013.

Arora, V. K. and Boer, G. J.: Uncertainties in the 20th century carbon budget associated with land use change, Glob. Chang. Biol., 16(12), 3327–3348, doi:10.1111/j.1365-2486.2010.02202.x, 2010.

Bentsen, M., Bethke, I., Debernard, J. B., Iversen, T., Kirkevåg, A., Seland, Ø., Drange, H., Roelandt, C., Seierstad, I. A., Hoose, C. and Kristjánsson, J. E.: The Norwegian Earth System Model, NorESM1-M – Part 1: Description and basic evaluation of the physical climate, Geosci. Model Dev., 6(3), 687–720, doi:10.5194/gmd-6-687-2013, 2013.

Bishop, C. H. and Abramowitz, G.: Climate model dependence and the replicate Earth paradigm, Clim. Dyn., 41(3-4), 885–900, doi:10.1007/s00382-012-1610-y, 2012.

Canadell, J. G., Le Quéré, C., Raupach, M. R., Field, C. B., Buitenhuis, E. T., Ciais, P., Conway, T. J., Gillett, N. P., Houghton, R. A. and Marland, G.: Contributions to accelerating atmospheric CO2 growth from economic activity, carbon intensity, and efficiency of natural sinks., Proc. Natl. Acad. Sci. U. S. A., 104(47), 18866–70, doi:10.1073/pnas.0702737104, 2007.

Chylek, P., Li, J., Dubey, M. K., Wang, M. and Lesins, G.: Observed and model simulated 20th century Arctic temperature variability: Canadian Earth System Model CanESM2, Atmos. Chem. Phys. Discuss., 11(8), 22893–22907, doi:10.5194/acpd-11-22893-2011, 2011.

Clark, D. B., Mercado, L. M., Sitch, S., Jones, C. D., Gedney, N., Best, M. J., Pryor, M., Rooney, G. G., Essery, R. L. H., Blyth, E., Boucher, O., Harding, R. J., Huntingford, C. and Cox, P. M.: The Joint UK Land Environment Simulator (JULES), model description – Part 2: Carbon fluxes and vegetation dynamics, Geosci. Model Dev., 4(3), 701–722, doi:10.5194/gmd-4-701-2011, 2011.

Collins, W. J., Bellouin, N., Doutriaux-Boucher, M., Gedney, N., Halloran, P., Hinton, T., Hughes, J., Jones, C. D., Joshi, M., Liddicoat, S., Martin, G., O'Connor, F., Rae, J., Senior, C., Sitch, S., Totterdell, I., Wiltshire, A. and Woodward, S.: Development and evaluation of an Earth-System model – HadGEM2, Geosci. Model Dev., 4(4), 1051–1075, doi:10.5194/gmd-4-1051-2011, 2011.

Cox, P. M.: Description of the TRIFFID dynamic global vegetation model, Met Office Hadley Centre Tech. Note, 24, 17pp, 2001.

Davidson, E. A. and Janssens, I. A.: Temperature sensitivity of soil carbon decomposition and feedbacks to climate change, Nature, 440(7081), 165–173, doi:10.1038/nature04514, 2006.

Doney, S. C., Lindsay, K., Fung, I. and John, J.: Natural Variability in a Stable, 1000-Yr Global Coupled Climate–Carbon Cycle Simulation, J. Clim., 19(13), 3033–3054, doi:10.1175/JCLI3783.1, 2006.

Dufresne, J.-L., Foujols, M.-A., Denvil, S., Caubel, A., Marti, O., Aumont, O., Balkanski, Y., Bekki, S., Bellenger, H., Benshila, R., Bony, S., Bopp, L., Braconnot, P., Brockmann, P., Cadule, P., Cheruy, F., Codron, F., Cozic, A., Cugnet, D., Noblet, N., Duvel, J.-P., Ethé, C., Fairhead, L., Fichefet, T., Flavoni, S., Friedlingstein, P., Grandpeix, J.-Y., Guez, L., Guilyardi, E., Hauglustaine, D., Hourdin, F., Idelkadi, A., Ghattas, J., Joussaume, S., Kageyama, M., Krinner, G., Labetoulle, S., Lahellec, A., Lefebvre, M.-P., Lefevre, F., Levy, C., Li, Z. X., Lloyd, J., Lott, F., Madec, G., Mancip, M., Marchand, M., Masson, S., Meurdesoif, Y., Mignot, J., Musat, I., Parouty, S., Polcher, J., Rio, C., Schulz, M., Swingedouw, D., Szopa, S., Talandier, C., Terray, P., Viovy, N. and Vuichard, N.: Climate change projections using the IPSL-CM5 Earth System Model: from CMIP3 to CMIP5, Clim. Dyn., 40(9-10), 2123–2165, doi:10.1007/s00382-012-1636-1, 2013.

Dunne, J. P., John, J. G., Adcroft, A. J., Griffies, S. M., Hallberg, R. W., Shevliakova, E., Stouffer, R. J., Cooke, W., Dunne, K. A., Harrison, M. J., Krasting, J. P., Malyshev, S. L., Milly, P. C. D., Phillipps, P. J., Sentman, L. T., Samuels, B. L., Spelman, M. J., Winton, M., Wittenberg, A. T. and Zadeh, N.: GFDL's ESM2 Global Coupled Climate–Carbon Earth System Models. Part I: Physical Formulation and Baseline Simulation Characteristics, J. Clim., 25(19), 6646–6665, doi:10.1175/JCLI-D-11-00560.1, 2012.

Exbrayat, J.-F., Pitman, A. J., Abramowitz, G. and Wang, Y.-P.: Sensitivity of net ecosystem exchange and heterotrophic respiration to parameterization uncertainty, J. Geophys. Res. Atmos., 118(4), 1640–1651, doi:10.1029/2012JD018122, 2013a.

Exbrayat, J.-F., Pitman, A. J., Zhang, Q., Abramowitz, G. and Wang, Y.-P.: Examining soil carbon uncertainty in a global model: response of microbial decomposition to temperature, moisture and nutrient limitation, Biogeosciences, 10(11), 7095–7108, doi:10.5194/bg-10-7095-2013, 2013b.

Exbrayat, J.-F., Pitman, A. J., and Abramowitz, G.: Disentangling residence time and temperature sensitivity of microbial decomposition in a global soil carbon model, Biogeosciences Discuss., 11, 4995-5021, doi:10.5194/bgd-11-4995-2014, 2014.

Falloon, P., Jones, C. D., Ades, M. and Paul, K.: Direct soil moisture controls of future global soil carbon changes: An important source of uncertainty, Global Biogeochem. Cycles, 25, GB3010, doi:201110.1029/2010GB003938, 2011.

FAO/IIASA/ISRIC/ISSCAS/JRC: Harmonized World Soil Database (version 1.21). FAO, Rome, Italy and IIASA, Laxenburg, Austria, 2012.

Foley, J. A.: An equilibrium model of the terrestrial carbon budget, Tellus B, 47(3), 310–319, doi:10.1034/j.1600-0889.47.issue3.3.x, 1995.

Friedlingstein, P., Meinshausen, M., Arora, V. K., Jones, C. D., Anav, A., Liddicoat, S. K. and Knutti, R.: Uncertainties in CMIP5 Climate Projections due to Carbon Cycle Feedbacks, J. Clim., 27(2), 511–526, doi:10.1175/JCLI-D-12-00579.1, 2014.

Friend, A. D., Lucht, W., Rademacher, T. T., Keribin, R., Betts, R., Cadule, P., Ciais, P., Clark, D. B., Dankers, R., Falloon, P. D., Ito, A., Kahana, R., Kleidon, A., Lomas, M. R., Nishina, K., Ostberg, S., Pavlick, S., Peylin, P., Schaphoff, S., Vuichard, N., Warszawski, L., Wiltshire, A., and Woodward, F. I.:Carbon residence time dominates uncertainty in terrestrial vegetation 508 responses to future climate and atmospheric CO_2, Proc. Natl. Acad. Sci., 111(9), 3280-3285, doi:10.1073/pnas.1222477110, 2014.

Gent, P. R., Danabasoglu, G., Donner, L. J., Holland, M. M., Hunke, E. C., Jayne, S. R., Lawrence, D. M., Neale, R. B., Rasch, P. J., Vertenstein, M., Worley, P. H., Yang, Z.-L. and Zhang, M.: The Community Climate System Model Version 4, J. Clim., 24(19), 4973–4991, doi:10.1175/2011JCLI4083.1, 2011.

Giorgetta, M. A., Jungclaus, J., Reick, C. H., Legutke, S., Bader, J., Böttinger, M., Brovkin, V., Crueger, T., Esch, M., Fieg, K., Glushak, K., Gayler, V., Haak, H., Hollweg, H.-D., Ilyina, T., Kinne, S., Kornblueh, L., Matei, D., Mauritsen, T., Mikolajewicz, U., Mueller, W., Notz, D., Pithan, F., Raddatz, T., Rast, S., Redler, R., Roeckner, E., Schmidt, H., Schnur, R., Segschneider, J., Six, K. D., Stockhause, M., Timmreck, C., Wegner, J., Widmann, H., Wieners, K.-H., Claussen, M., Marotzke, J. and Stevens, B.: Climate and carbon cycle changes from 1850 to 2100 in MPI-ESM simulations for the Coupled Model Intercomparison Project phase 5, J. Adv. Model. Earth Syst., 5(3), 572–597, doi:10.1002/jame.20038, 2013.

Hugelius, G., Tarnocai, C., Broll, G., Canadell, J. G., Kuhry, P., and Swanson, D. K.: The Northern Circumpolar Soil Carbon Database: spatially distributed datasets of soil coverage and soil carbon storage in the northern permafrost regions, Earth Syst. Sci. Data, 5, 3-13, doi:10.5194/essd-5-3-2013, 2013.

366 Ito, A.: A historical meta-analysis of global terrestrial net primary productivity: are estimates
367 converging? Glob. Change Biol., 17, 3161–3175, doi:10.1111/j.1365-2486.2011.02450.x, 2011.

368 Jenkinson, D. S.: The turnover of organic-carbon and nitrogen in soil, Philos. T. R. Soc. Lond., 329,
369 361–368, 1990.

370 Ji, J., Huang, M. and Li, K.: Prediction of carbon exchanges between China terrestrial ecosystem
371 and atmosphere in 21st century, Sci. China Ser. D Earth Sci., 51(6), 885–898, doi:10.1007/s11430-
372 008-0039-y, 2008.

373 Jobbágy, E. G. and Jackson, R. B.: The vertical distribution of soil organic carbon and its relation to
374 climate and vegetation, Ecol. Appl., 10(2), 423–436, doi:10.1890/1051-
375 0761(2000)010[0423:TVDOSO]2.0.CO;2, 2000.

376 Kirschbaum, M. U. F.: Soil respiration under prolonged soil warming: are rate reductions caused by
377 acclimation or substrate loss?, Glob. Chang. Biol., 10(11), 1870–1877, doi:10.1111/j.1365-
378 2486.2004.00852.x, 2004.

379 Knorr, W.: Annual and interannual CO2 exchanges of the terrestrial biosphere: process-based
380 simulations and uncertainties, Glob. Ecol. Biogeogr., 9(3), 225–252, doi:10.1046/j.1365-
381 2699.2000.00159.x, 2000.

382 Knorr, W., Prentice, I. C., House, J. I. and Holland, E. A.: Long-term sensitivity of soil carbon
383 turnover to warming, Nature, 433(7023), 298–301, doi:10.1038/nature03226, 2005.

384 Krinner, G., Viovy, N., de Noblet-Ducoudré, N., Ogée, J., Polcher, J., Friedlingstein, P., Ciais, P.,
385 Sitch, S. and Prentice, I. C.: A dynamic global vegetation model for studies of the coupled
386 atmosphere-biosphere system, Global Biogeochem. Cycles, 19(1), GB1015,
387 doi:10.1029/2003GB002199, 2005.

388 Lawrence, D. M., Oleson, K. W., Flanner, M. G., Thornton, P. E., Swenson, S. C., Lawrence, P. J.,
389 Zeng, X., Yang, Z.-L., Levis, S., Sakaguchi, K., Bonan, G. B. and Slater, A. G.: Parameterization
390 improvements and functional and structural advances in Version 4 of the Community Land Model,
391 J. Adv. Model. Earth Syst., 3(3), M03001, doi:10.1029/2011MS000045, 2011.

392 Lloyd, J. and Taylor, J. A.: On the Temperature Dependence of Soil Respiration, Funct. Ecol., 8,
393 315–323, 1994.

Lund, M., Lafleur, P. M., Roulet, N. T., Lindroth, A., Christensen, T. R., Aurela, M., Chojnicki, B. H., Flanagan, L. B., Humphreys, E. R., Laurila, T., Oechel, W. C., Olejnik, J., Rinne, J., Schubert, P. and Nilsson, M. B.: Variability in exchange of CO2 across 12 northern peatland and tundra sites, Glob. Chang. Biol., no–no, doi:10.1111/j.1365-2486.2009.02104.x, 2009.

Luo, Y., Wan, S., Hui, D. and Wallace, L. L.: Acclimatization of soil respiration to warming in a tall grass prairie., Nature, 413(6856), 622–5, doi:10.1038/35098065, 2001.

Nishina, K., Ito, A., Beerling, D. J., Cadule, P., Ciais, P., Clark, D. B., Falloon, P., Friend, A. D., Kahana, R., Kato, E., Keribin, R., Lucht, W., Lomas, M., Rademacher, T. T., Pavlick, R., Schaphoff, S., Vuichard, N., Warszawaski, L. and Yokohata, T.: Quantifying uncertainties in soil carbon responses to changes in global mean temperature and precipitation, Earth Syst. Dyn., 5(1), 197–209, doi:10.5194/esd-5-197-2014, 2014.

Parton, W. J., Schimel, D. S., Cole, C. V. and Ojima, D. S.: Analysis of Factors Controlling Soil Organic Matter Levels in Great Plains Grasslands1, Soil Sci. Soc. Am. J., 51(5), 1173-1179, doi:10.2136/sssaj1987.03615995005100050015x, 1987.

Parton, W. J., Stewart, J. W. B. and Cole, C. V.: Dynamics of C, N, P and S in grassland soils: a model, Biogeochemistry, 5(1), 109–131, doi:10.1007/BF02180320, 1988.

Le Quéré, C., Raupach, M. R., Canadell, J. G., Marland, G., Bopp, L., Ciais, P., Conway, T. J., Doney, S. C., Feely, R. A., Foster, P., Friedlingstein, P., Gurney, K., Houghton, R. A., House, J. I., Huntingford, C., Levy, P. E., Lomas, M. R., Majkut, J., Metzl, N., Ometto, J. P., Peters, G. P., Prentice, I. C., Randerson, J. T., Running, S. W., Sarmiento, J. L., Schuster, U., Sitch, S., Takahashi, T., Viovy, N., van der Werf, G. R. and Woodward, F. I.: Trends in the sources and sinks of carbon dioxide, Nat. Geosci., 2(12), 831–836, doi:10.1038/ngeo689, 2009.

Raddatz, T. J., Reick, C. H., Knorr, W., Kattge, J., Roeckner, E., Schnur, R., Schnitzler, K.-G., Wetzel, P. and Jungclaus, J.: Will the tropical land biosphere dominate the climate–carbon cycle feedback during the twenty-first century?, Clim. Dyn., 29(6), 565–574, doi:10.1007/s00382-007-0247-8, 2007.

Randerson, J. T., Thompson, M. V., Conway, T. J., Fung, I. Y. and Field, C. B.: The contribution of terrestrial sources and sinks to trends in the seasonal cycle of atmospheric carbon dioxide, Global Biogeochem. Cycles, 11(4), 535–560, doi:10.1029/97GB02268, 1997.

Sato, H., Itoh, A. and Kohyama, T.: SEIB–DGVM: A new Dynamic Global Vegetation Model using a spatially explicit individual-based approach, Ecol. Modell., 200(3-4), 279–307, doi:10.1016/j.ecolmodel.2006.09.006, 2007.

Schmidt, M. W. I., Torn, M. S., Abiven, S., Dittmar, T., Guggenberger, G., Janssens, I. A., Kleber, M., Kögel-Knabner, I., Lehmann, J., Manning, D. A. C., Nannipieri, P., Rasse, D. P., Weiner, S. and Trumbore, S. E.: Persistence of soil organic matter as an ecosystem property., Nature, 478(7367), 49–56, doi:10.1038/nature10386, 2011.

Shangguan, W., Dai, Y., Duan, Q., Liu, B., Yuan, H.: A global soil data set for earth system modeling, J. Adv. Model. Earth Syst., 6, 249–263, doi:10.1002/2013MS000293, 2014.

Shevliakova, E., Pacala, S. W., Malyshev, S., Hurtt, G. C., Milly, P. C. D., Caspersen, J. P., Sentman, L. T., Fisk, J. P., Wirth, C. and Crevoisier, C.: Carbon cycling under 300 years of land use change: Importance of the secondary vegetation sink, Global Biogeochem. Cycles, 23(2), GB2022, doi:10.1029/2007GB003176, 2009.

Shindell, D. T., Pechony, O., Voulgarakis, A., Faluvegi, G., Nazarenko, L., Lamarque, J.-F., Bowman, K., Milly, G., Kovari, B., Ruedy, R. and Schmidt, G. A.: Interactive ozone and methane chemistry in GISS-E2 historical and future climate simulations, Atmos. Chem. Phys., 13(5), 2653–2689, doi:10.5194/acp-13-2653-2013, 2013.

Taylor, K. E., Stouffer, R. J. and Meehl, G. A.: An overview of CMIP5 and the experiment design, Bull. Am. Meteorol. Soc., 93(4), 485–498, doi:10.1175/BAMS-D-11-00094.1, 2012.

Thornton, P. E., Lamarque, J.-F., Rosenbloom, N. A. and Mahowald, N. M.: Influence of carbon-nitrogen cycle coupling on land model response to CO 2 fertilization and climate variability, Global Biogeochem. Cycles, 21(4), GB4018, doi:10.1029/2006GB002868, 2007.

Thornton, P. E. and Rosenbloom, N. A.: Ecosystem model spin-up: Estimating steady state conditions in a coupled terrestrial carbon and nitrogen cycle model, Ecol. Modell., 189(1-2), 25–48, doi:10.1016/j.ecolmodel.2005.04.008, 2005.

Todd-Brown, K. E. O., Randerson, J. T., Post, W. M., Hoffman, F. M., Tarnocai, C., Schuur, E. a. G. and Allison, S. D.: Causes of variation in soil carbon simulations from CMIP5 Earth system models and comparison with observations, Biogeosciences, 10(3), 1717–1736, doi:10.5194/bg-10-1717-2013, 2013.

Warszawski, L., Frieler, K., Huber, V., Piontek, F., Serdeczny, O. and Schewe, J.: The Inter-Sectoral Impact Model Intercomparison Project (ISI-MIP): project framework., Proc. Natl. Acad. Sci. U. S. A., 111(9), 3228–32, doi:10.1073/pnas.1312330110, 2014.

Watanabe, S., Hajima, T., Sudo, K., Nagashima, T., Takemura, T., Okajima, H., Nozawa, T., Kawase, H., Abe, M., Yokohata, T., Ise, T., Sato, H., Kato, E., Takata, K., Emori, S. and Kawamiya, M.: MIROC-ESM 2010: model description and basic results of CMIP5-20c3m experiments, Geosci. Model Dev., 4(4), 845–872, doi:10.5194/gmd-4-845-2011, 2011.

Wieder, W. R., Bonan, G. B. and Allison, S. D.: Global soil carbon projections are improved by modelling microbial processes, Nat. Clim. Chang., 3(10), 909–912, doi:10.1038/nclimate1951, 2013.

Wu, T., Li, W., Ji, J., Xin, X., Li, L., Wang, Z., Zhang, Y., Li, J., Zhang, F., Wei, M., Shi, X., Wu, F., Zhang, L., Chu, M., Jie, W., Liu, Y., Wang, F., Liu, X., Li, Q., Dong, M., Liang, X., Gao, Y. and Zhang, J.: Global carbon budgets simulated by the Beijing Climate Center Climate System Model for the last century, J. Geophys. Res. Atmos., 118(10), 4326–4347, doi:10.1002/jgrd.50320, 2013.

Xenakis, G. and Williams, M.: Comparing microbial and chemical kinetics for modelling soil organic carbon decomposition using the DecoChem v1.0 and DecoBio v1.0 models, Geosci. Model Dev., 7, 1519-1533, doi:10.5194/gmd-7-1519-2014, 2014.

Xia, J., Luo, Y., Wang, Y.-P. and Hararuk, O.: Traceable components of terrestrial carbon storage capacity in biogeochemical models., Glob. Chang. Biol., 19(7), 2104–16, doi:10.1111/gcb.12172, 2013.

Xia, J. Y., Luo, Y. Q., Wang, Y.-P., Weng, E. S. and Hararuk, O.: A semi-analytical solution to accelerate spin-up of a coupled carbon and nitrogen land model to steady state, Geosci. Model Dev., 5(5), 1259–1271, doi:10.5194/gmd-5-1259-2012, 2012.

Tables

Table 1. CMIP5 models and number of simulations used in this paper for historical and RCP 8.5 runs. The first column provides the letter code used in the figures. References and details about soil carbon components are provided in supplementary Tables 2 and 3.

	Model name	Institution	Number of model runs	
			Historical	RCP 8.5
A	BCC-CSM1.1	Beijing Climate Center (China)	3	0
B	CanESM2	Canadian Centre for Climate Modelling and Analysis (Canada)	5	5
C	CCSM4	National Center for Atmospheric Research (USA)	6	6
D	GFDL-ESM2G	Geophysical Fluid Dynamics Laboratory (USA)	1	1
E[a]	GISS-E2-H	NASA Goddard Institute for Space Studies (USA)	17	3
	GISS-E2-R		25	3
F[a]	HadGEM2-CC	Met Office/Hadley Centre (UK)	1	1
	HadGEM2-ES		3	3
G[a]	IPSL-CM5A-LR	Institut Pierre Simon Laplace (France)	6	4
	IPSL-CM5B-LR		1	1
H[a]	MIROC-ESM	Japan Agency for Marine-Earth Science and Technology (Japan)	3	1
	MIROC-ESM-CHEM		1	1
I	MPI-ESM-LR	Max Planck Institute (Germany)	3	3
J[a]	NorESM1-M	Bjerknes Centre for Climate Research (Norway)	3	1
	NorESM1-ME		1	1

[a]models from the same institution where averaged to avoid pseudo-replication

482 **Table 2.** Details about the CMIP5 models terrestrial and soil component and associated references.

	Model name	Terrestrial component	Soil biogeochemistry	# of pools		N limitations
				L	S	
A	BCC-CSM1.1 (Wu et al., 2013)	AVIM2 (Ji et al., 2008)	Based on CENTURY (Parton et al., 1987)	2	6	Yes
B	CanESM2 (Chylek et al., 2011)	CTEM (Arora and Boer, 2010)	CTEM (Arora and Boer, 2010)	1	1	No
C	CCSM4 (Gent et al., 2011)	CLM4-CN (Lawrence et al., 2011)	CN module (Thornton et al., 2007) based on Biome-BGC 4.1.2 (Thornton and Rosenbloom, 2005)	3	3	Yes
D	GFDL-ESM2G (Dunne et al., 2012)	LM3.0 (Shevliakova et al., 2009)	Based on CENTURY (Parton et al., 1987)	–	2	No
E	GISS-E2 (Shindell et al., 2013)	NCAR-CSM1.4 (Doney et al., 2006)	Based on CASA (Randerson et al., 1997)	–	9	No
F	HadGEM2 (Collins et al., 2011)	JULES (Clark et al., 2011)	Based on TRIFFID (Cox, 2001) and RothC (Jenkinson, 1990)	–	4	No
G	IPSL-CM5 (Dufresne et al., 2013)	ORCHIDEE	STOMATE (Krinner et al., 2005) and CENTURY (Parton et al., 1988)	3	4	No
H	MIROC-ESM (Watanabe et al., 2011)	SEIB-DGVM (Sato et al., 2007)	Based on DEMETER-1 (Foley et al., 2005)	–	2	No
I	MPI-ESM-LR (Giorgetta et al., 2013)	JSBACH (Raddatz et al., 2007)	Based on Bethy (Knorr, 2000) and CENTURY (Parton et al., 1988)	1	1	No

J	NorESM1 (Bentsen et al., 2012)	CLM4-CN (Lawrence et al., 2011)	CN module (Thornton et al., 2007) based on Biome-BGC 4.1.2 (Thornton and Rosenbloom, 2005)	3	3	Yes

485 **Table 3.** Model specific values of SOC_{in}, R_h and SOC used in Figures 1 to 4. Values are averaged over the indicated years. All data are
486 rounded to whole numbers. Values for 2091-2100 are from the Representative Concentration Pathway 8.5 (RCP 8.5) simulations.

Model	SOC_{in} [Pg C yr^{-1}]			R_h [Pg C yr^{-1}]			Total soil carbon [Pg C]		
	1861-1870	1996-2005	2091-2100	1861-1870	1996-2005	2091-2100	1861-1870	1996-2005	2091-2100
A	75	87	–	75	86	–	1273	1351	–
B	57	64	84	56	65	85	1511	1541	1490
C	46	49	56	46	49	57	563	576	582
D	79	85	119	79	86	120	1798	1781	1785
E	45	55	58	45	55	61	2113	2306	2118
F	67	86	140	67	84	137	1178	1287	1596
G	76	87	123	76	87	123	1598	1626	1709
H	57	59	71	56	55	74	2515	2566	2494
I	66	75	100	66	74	99	2938	3047	3266
J	52	55	61	52	55	62	650	666	654

Figure legends

Figure 1. Relationship between total *SOC* in CMIP5 models at two different times: modern stocks as a function of pre-industrial stocks (upper panel), future stocks as a function of modern stocks (middle panel) and future stocks as a function of pre-industrial stocks (lower panel). Letters correspond to models as in Table 1 and models in green (i.e. C and J) integrate nitrogen limitation. The gray area is the 95% confidence interval of modern total *SOC* derived from the HWSD. Equation, R^2 and p values correspond to the linear relationship between stocks built using data from all models (solid line). The dotted line is the 1:1 line.

Figure 2. Relationship between pre-industrial global *SOC* input and pre-industrial R_h. Letters are the same as in Table 1 and models in green (i.e. C and J) integrate nitrogen limitation. The solid line is a linear relationship constructed using all models with equation, R^2 and p values indicated in the top left corner. The dashed line represents the 1:1 relationship.

Figure 3. Relationship between pre-industrial *SOC* input and pre-industrial total *SOC* stocks at the beginning of the historical experiment. Letters correspond to the same models as in Table 1 and models in green (i.e. C and J) integrate nitrogen limitation. The solid line is a linear relationship constructed using all models with equation, R^2 and p values indicated in the top left corner.

Figure 4. Relationship between pre-industrial global *SOC* residence time and total *SOC*. Letters correspond to the same models as in Table 1 and models in green (i.e. C and J) integrate nitrogen limitation. The solid line is a linear relationship constructed using all models with equation, R^2 and p values indicated in the top left corner.

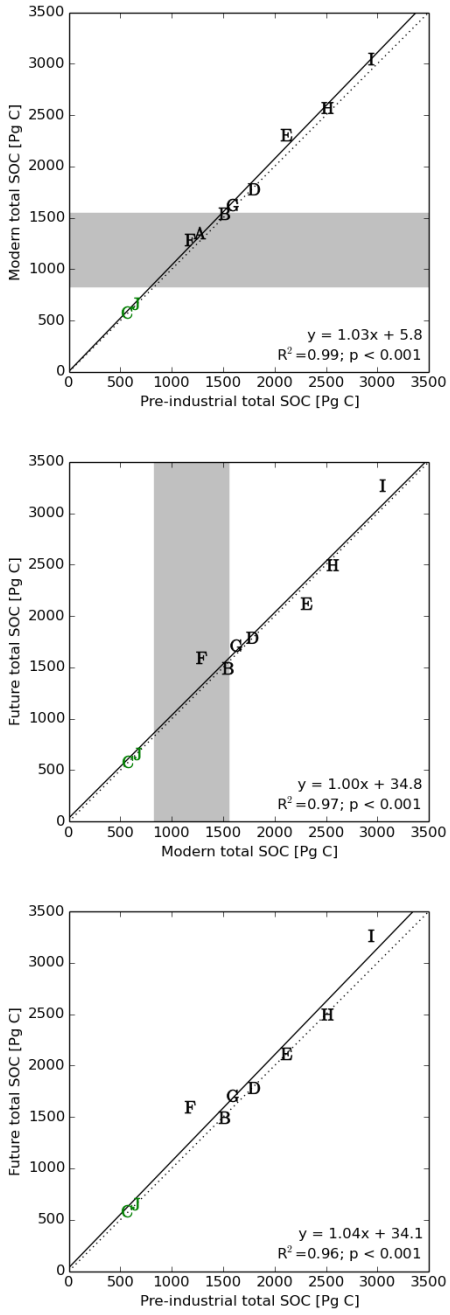

512

513 **Figure 1.** Relationship between total *SOC* in CMIP5 models at two different times: modern
514 stocks as a function of pre-industrial stocks (upper panel), future stocks as a function of
515 modern stocks (middle panel) and future stocks as a function of pre-industrial stocks (lower
516 panel). Letters correspond to models as in Table 1 and models in green (i.e. C and J) integrate
517 nitrogen limitation. The gray area is the 95% confidence interval of modern total *SOC* derived
518 from the HWSD. Equation, R^2 and p values correspond to the linear relationship between
519 stocks built using data from all models (solid line). The dotted line is the 1:1 line.

520

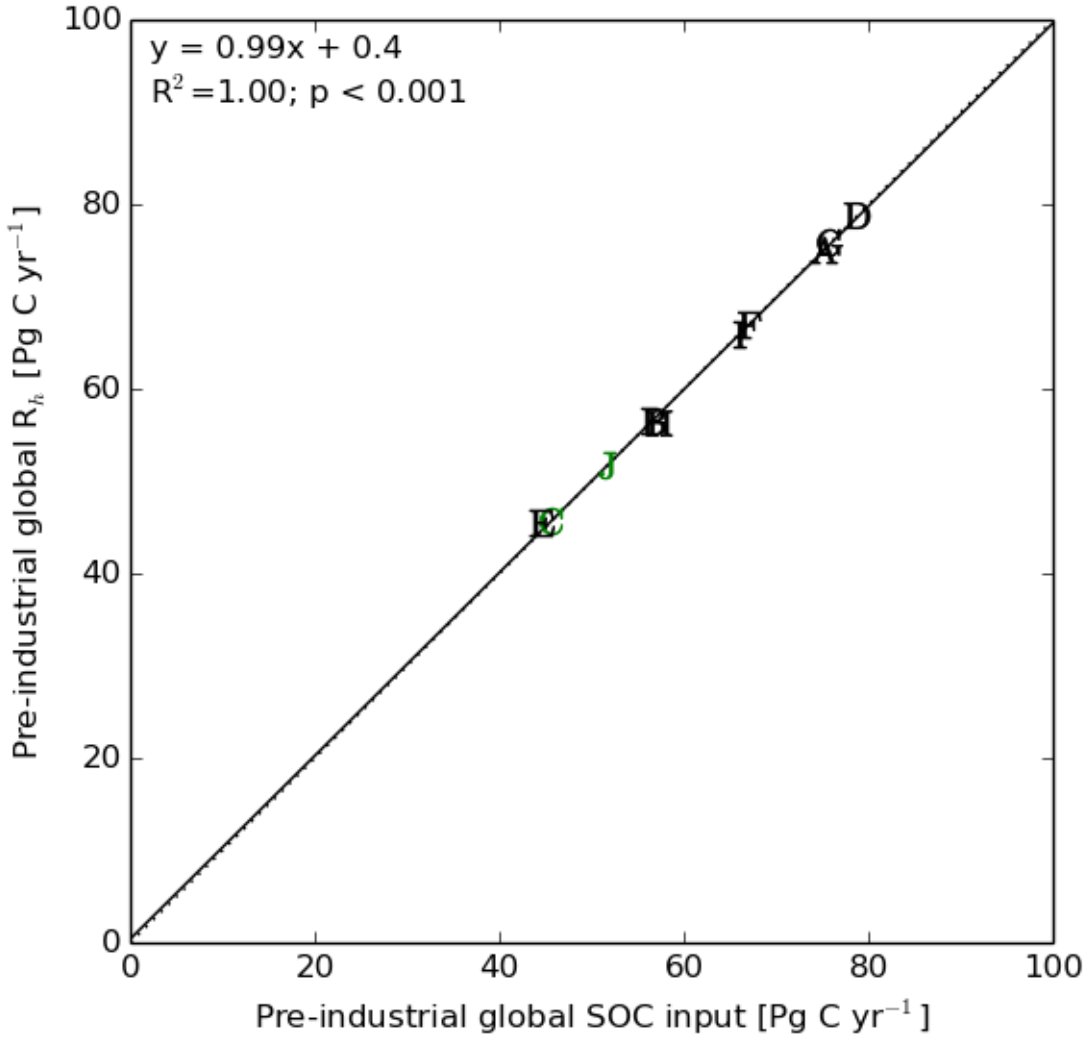

Figure 2. Relationship between pre-industrial global *SOC* input and pre-industrial R_h. Letters are the same as in Table 1 and models in green (i.e. C and J) integrate nitrogen limitation. The solid line is a linear relationship constructed using all models with equation, R^2 and p values indicated in the top left corner. The dashed line represents the 1:1 relationship.

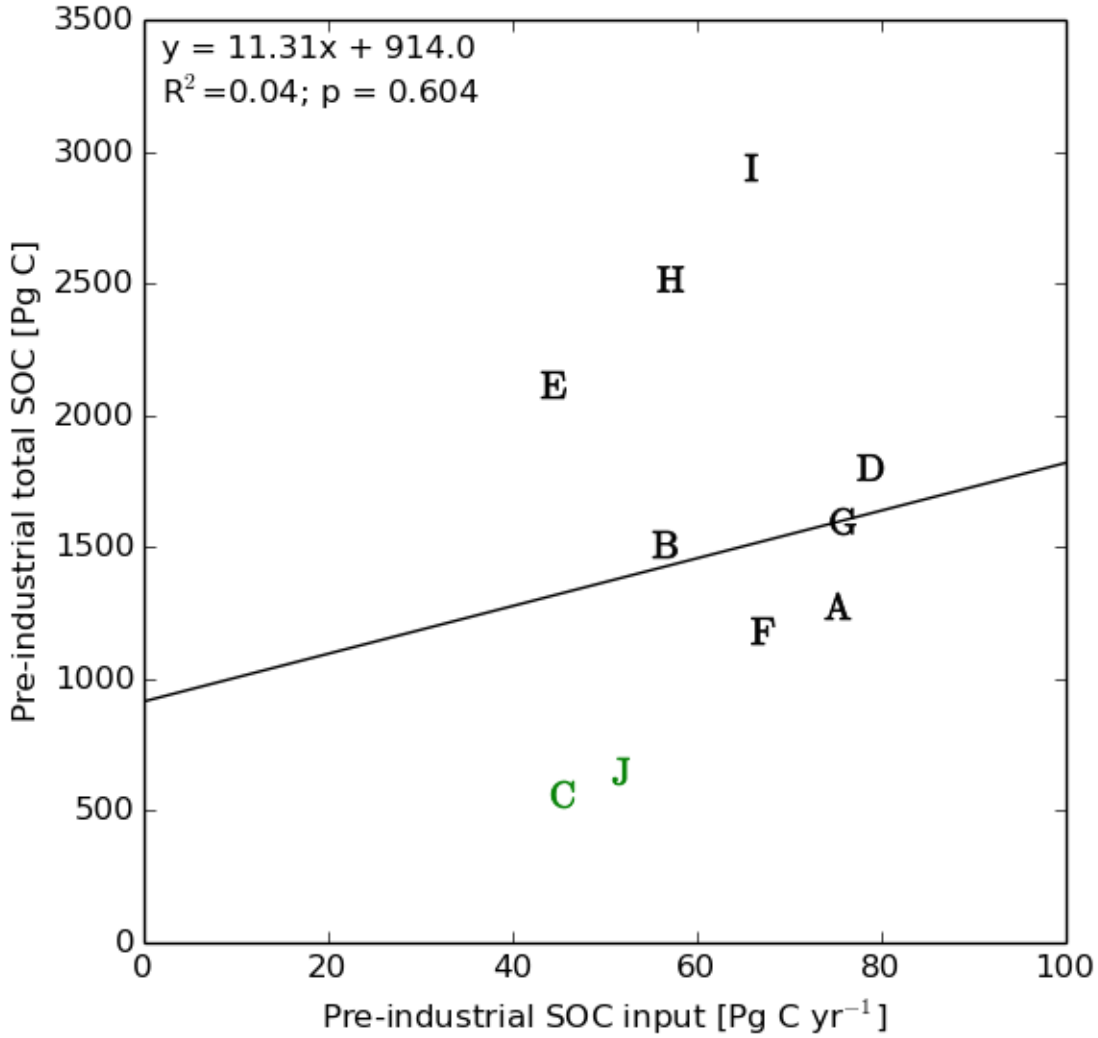

Figure 3. Relationship between pre-industrial *SOC* input and pre-industrial total *SOC* stocks at the beginning of the historical experiment. Letters correspond to the same models as in Table 1 and models in green (i.e. C and J) integrate nitrogen limitation. The solid line is a linear relationship constructed using all models with equation, R^2 and p values indicated in the top left corner.

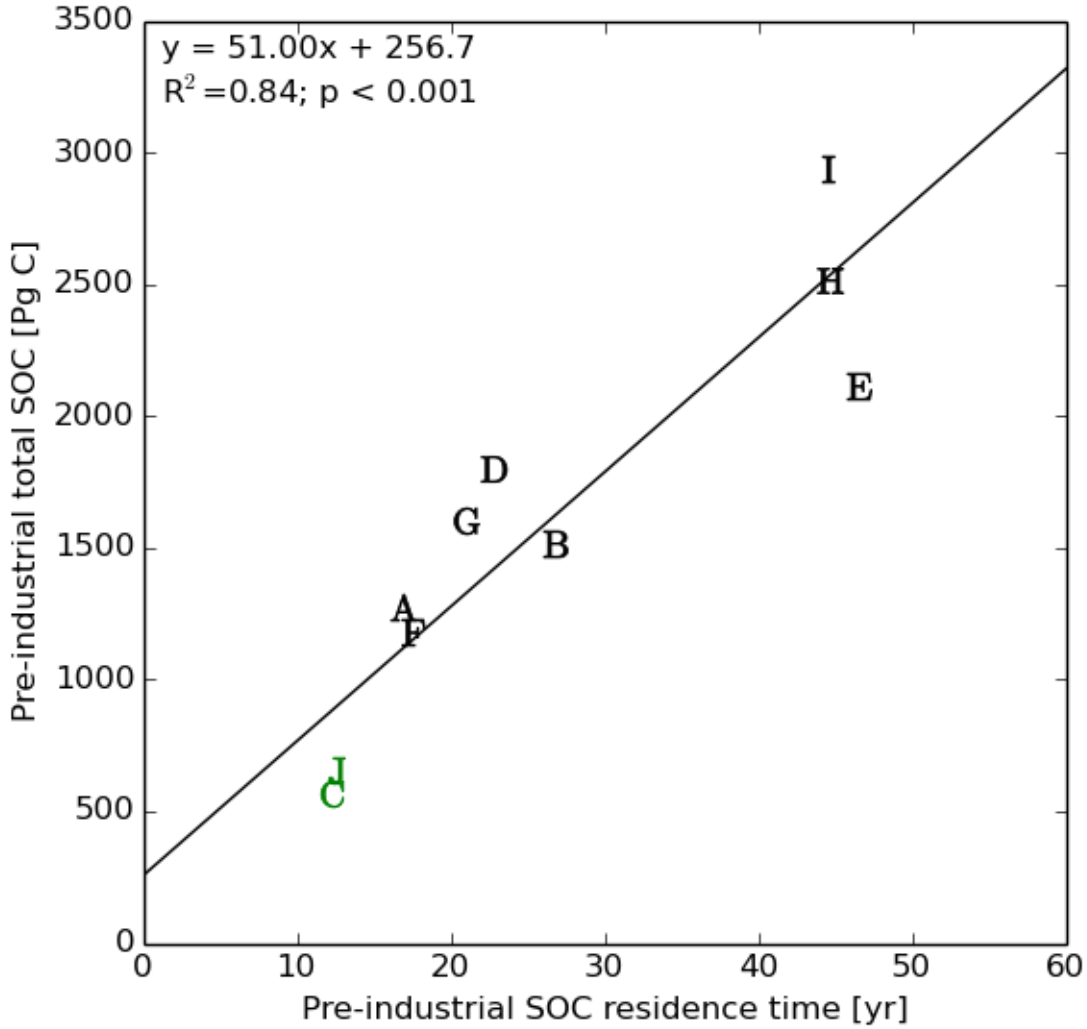

Figure 4. Relationship between pre-industrial global *SOC* residence time and total *SOC*. Letters correspond to the same models as in Table 1 and models in green (i.e. C and J) integrate nitrogen limitation. The solid line is a linear relationship constructed using all models with equation, R^2 and p values indicated in the top left corner.